

### 3.5.8

## TOF studies of multiple Bragg reflections in cylindrically bent perfect crystals at small pulsed neutron source

P Mikula<sup>1</sup> and M Furusaka<sup>2</sup>

<sup>1</sup>Nuclear Physics Institute ASCR, v.v.i., 25068 Řež, Czech Republic

<sup>2</sup>Faculty of Engineering, Hokkaido University, Sapporo, Hokkaido, 060-8628, Japan

E-mail: mikula@ujf.cas.cz

**Abstract.** It is well known that multiple Bragg reflections (MBR) realized in a bent-perfect crystal (BPC) slab can provide a monochromatic beam of excellent resolution parameters. The sets of different lattice planes participated in MBR effects that are mutually in dispersive diffraction geometry behave differently in comparison with the case of perfect nondeformed or mosaic crystals. Due to the elastic bending – homogeneous deformation – the kinematical approach can be applied in this MBR process. The homogeneous elastic deformation can enormously strengthen the MBR effects which can be then investigated even at small pulsed neutron sources. In this way, by using neutron diffraction and the TOF method carried out at the Hokkaido Linac neutron source many strong MBR reflections accompanying forbidden Si(222) of Si(002) ones can be observed. The advantage of the TOF method consists in the fact that not only primary MBR reflections related to the basic forbidden reflections could be observed but also their non-negligible higher orders which could be easily separated in the time-of-flight spectra.

### 1. Introduction

Using a conception of the reciprocal lattice space, MBR effects occur whenever two or more reciprocal lattice vectors lie on the surface of Ewald sphere simultaneously [1-4]. It means that a primary crystal lattice represented by a scattering vector  $\mathbf{g}_1$  is oriented with respect to the incident beam in such a way that more than one set of planes are simultaneously operative for a given wavelength (see figure 1). One of them may be described as an operative secondary reflection represented by a scattering vector  $\mathbf{g}_2$ . In fact there can be several secondary reflections. However, it follows from the crystal symmetry that when a secondary reflection fulfils the Bragg condition simultaneously with the primary one, there exists automatically the tertiary reflection represented by  $\mathbf{g}_3 = \mathbf{g}_1 - \mathbf{g}_2$  (see figure 2), which is co-operative with the secondary one. The vector sum  $\mathbf{g}_2 + \mathbf{g}_3$  then represents a double diffracted beam which has the same direction as the one that could have been reflected by the particular primary set of planes represented by the scattering vector  $\mathbf{g}_1$  ( $\mathbf{g}_1 = \mathbf{g}_2 + \mathbf{g}_3$ ). Thus, the MBR effects can result in a so called *Aufhellung* when reducing the intensity of a strong primary reflection or *Umweganregung* when increasing the intensity of a weak primary reflection. In the extreme case of the *Umweganregung* a positive diffraction intensity simulation of forbidden primary reflection can appear. Since the Renninger's first observation of the MBR-peaks many theoretical and experimental investigations of the generally n-beam cases mostly related to X-ray diffraction have been published (see e.g. [4]; in this book many related references can be found).

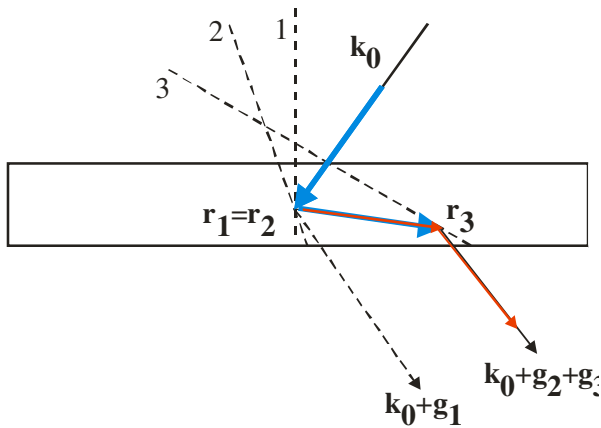


**Figure 1.** Schematic diagram of a two-step multiple Bragg reflection simulating a primary reflection. The numbers 1,2 and 3 represent the primary, secondary and tertiary reflection planes, respectively.

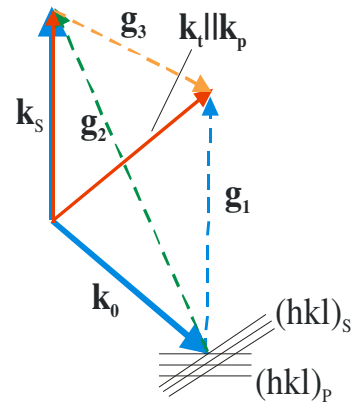


**Figure 2.** Schematic diagram of a two-step multiple Bragg reflection simulating a primary reflection in reciprocal space.

Concerning neutrons, relatively small MR-effects were observed in mosaic crystals [5-9]. Contrary to X-rays, in the case of perfect single crystals the flux of thermal neutrons at present neutron sources is usually not sufficient for the observation of such small dynamical diffraction effects. However, the situation is quite different in the case of neutron diffraction by elastically deformed perfect crystals [10-17]. In the related papers there is described an observation of a large strengthening of the MBR intensity of the monochromatic beam by ultrasonic vibrations and later by cylindrical bending. In this paper we show that the strengthening of the MBR effects by cylindrical bending is so strong that the effects can be effectively studied by the TOF method even at Linac based small neutron source (Hokkaido University, Sapporo).

## 2. Experimental details

For bringing more reciprocal lattice points on the Ewald sphere and the investigation of multiple reflection effects two methods are usually used:

- a. Method of azimuthal rotation of the crystal lattice around the scattering vector of the primary reflection for a fixed neutron (X-ray) wavelength (e.g. [16,17]).
- b. Method of  $\theta-2\theta_b$  scan in the white beam for a fixed azimuthal angle (e.g. [14,15]).  $\theta$  is the Bragg angle related to the primary reflection and  $2\theta_b$  is the scattering angle at which a point detector is set.

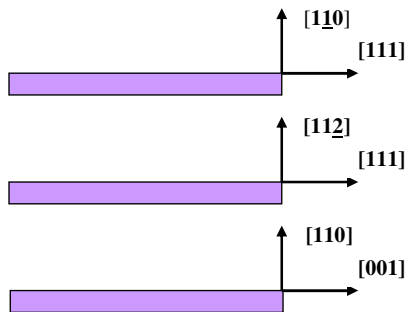


**Figure 3.** Three Si slabs of different cut were used in the experimental TOF investigation of chosen MBR effects.

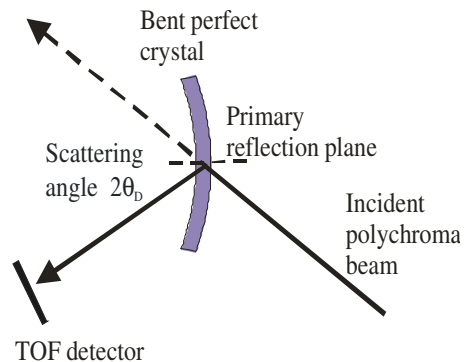


**Figure 4.** Schematic drawing of the experimental setting.

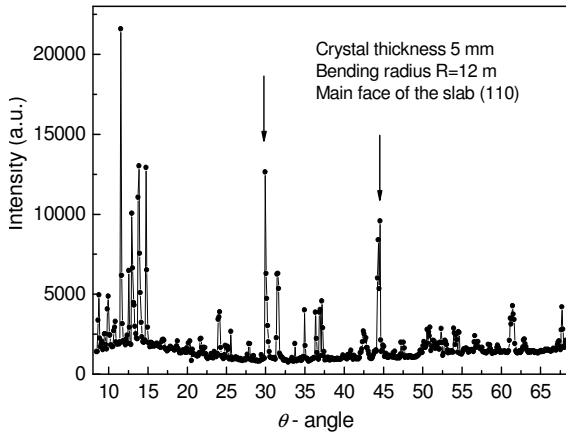


**Figure 5.** Part of the  $\theta-2\theta_D$  scan carried out by means of the crystal slab with the largest face parallel to  $(110)$  and set for  $(222)$  reflections.

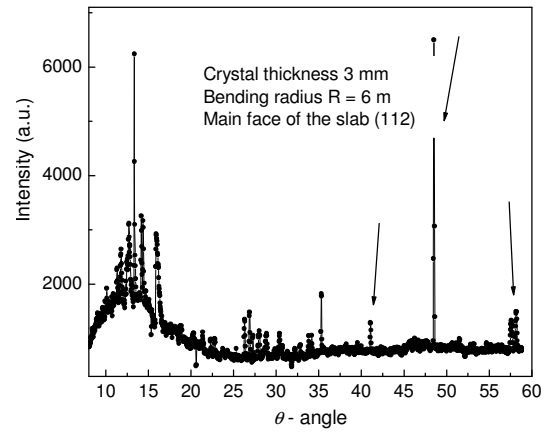


**Figure 6.** Part of the  $\theta-2\theta_D$  scan carried out by means of the crystal slab with the largest face parallel to  $(11\bar{2})$  and set for  $(222)$  reflections.

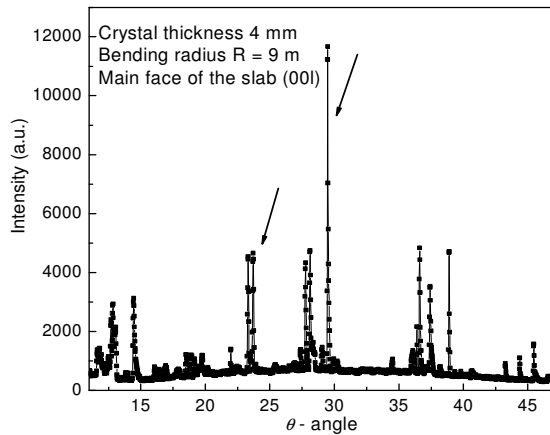


**Figure 7.** Part of the  $\theta-2\theta_D$  scan carried out by means of the crystal slab with the largest face parallel to  $(110)$  and set for  $(002)$  reflections.

However, if the polychromatic incident beam is impinging on the crystal which fulfils a MBR-condition for some primary reflection and the neutron wavelength  $\lambda$ , the related MBR-effect can be overlapped by the ones related to higher orders of  $\lambda/n$  ( $n$  is integer). It should be pointed out that the higher orders could be either allowed higher orders of primary reflections or higher orders of MBR-effects. For example, if the Si(222) crystal (forbidden reflection) is set in the Bragg reflection and also some other reciprocal points are on the Ewald sphere together with the  $\langle 222 \rangle$  one (which is one of our experimental cases), the obtained possible neutron diffraction signal may

consist of individual contributions coming from the allowed reflections Si(111), Si(333), Si(444) etc. as well as from MBR-effects accompanying Si(111), Si(222), Si(333), Si(444), etc. The symmetric transmission geometry has appeared to be the easiest diffraction geometry for MBR studies in the elastically deformed (cylindrically bent) perfect crystals where mutual orientation of the scattering vector  $\mathbf{g}$  with respect to the deformation vector  $\mathbf{u}$  plays an enormous role in the reflectivity properties of the deformed crystal. According to e.g. ref. 18 and 19 the integrated reflectivity of a deformed crystal is a function of the scalar product  $(\mathbf{g}\cdot\mathbf{u})$  which may be zero for both forbidden and its higher order reflections, i.e.  $(\mathbf{g}_1\cdot\mathbf{u})=0$ ,  $((\mathbf{g}_1/n)\cdot\mathbf{u})=0$ . It means that the corresponding integrated reflectivities are independent of the deformation represented by the displacement of atoms  $\mathbf{u}$  [20,21]. This is also valid for our chosen case of the cylindrical bending and symmetric transmission geometry. On the other hand  $(\mathbf{g}_2\cdot\mathbf{u}) = -(\mathbf{g}_3\cdot\mathbf{u})$  need not be zero and the deformation can bring about a large increase of the MBR-effect keeping the integrated reflectivity related to the primary reflection and higher order primary reflections constant at the value of the perfect

crystal. Therefore, for the investigation of the MBR- effects by the TOF method three Si slabs of different cut but all set in the symmetric transmission diffraction geometry were used (see figures 3 and 4). Several rather strong MBR effects already known from the earlier diffraction measurements carried out by the  $\theta-2\theta_D$  scanning in the white beam for a fixed azimuthal angle  $\phi=0^\circ$  have been chosen for these TOF studies. Parts of the related  $\theta-2\theta_D$  scans taken from ref. [14,15] where the chosen MBR effects for the TOF measurements are marked by arrows are shown in figures 5-7.

### 3. TOF experimental results

For indexing of the MBR-effects accompanying allowed or forbidden reflections we refer to the calculation procedures introduced e.g. in the papers [17,22,23]. Figures 8-10 show the calculated parts of the azimuth-Bragg angle relationships for the basic 222 and 002 primary reflections of the diamond structure and the chosen experimental points related to the MBR peaks labeled by arrows (see figures 5-7) are marked by circles. The indexes of individual lines in figures 8-10 correspond to the secondary reflections which can bring about the MBR effect

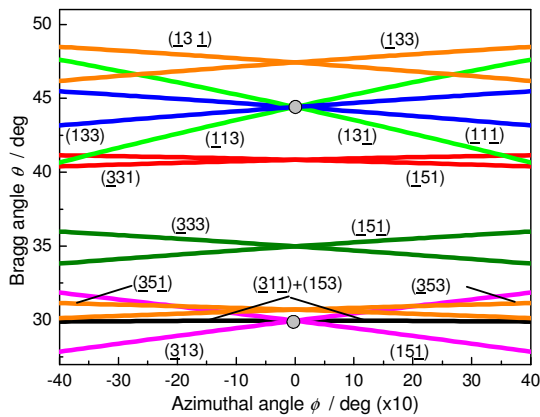


**Figure 8.** Part of the azimuth–Bragg angle relationships for the 222 primary reflections of the diamond structure for the slab having the main face parallel to  $(1\bar{1}0)$  planes.

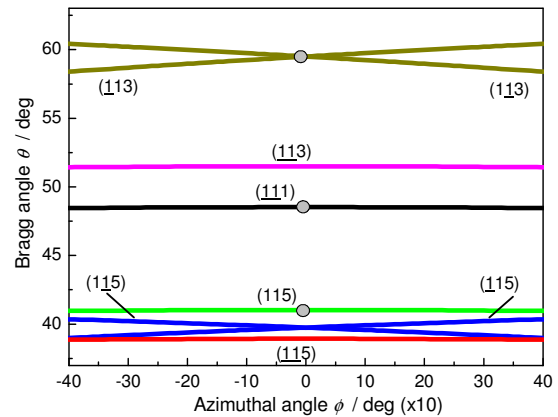


**Figure 9.** Part of the azimuth–Bragg angle relationships for the 222 primary reflections of the diamond structure for the slab having the main face parallel to  $(11\bar{2})$  planes.

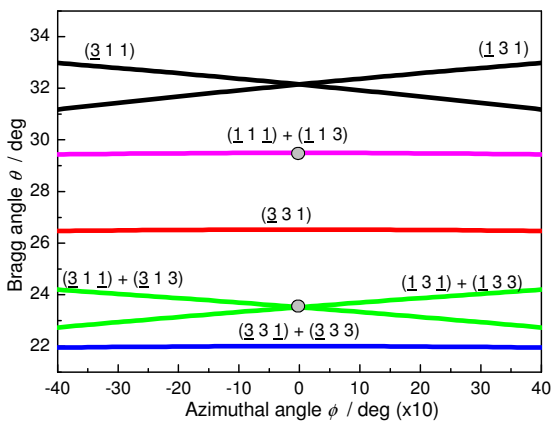


**Figure 10.** Part of the azimuth–Bragg angle relationships for the 002 primary reflections of the diamond structure for the slab having the main face parallel to  $(1\bar{1}0)$  planes.

with respect to the chosen primary reflection. The cooperative tertiary reflection can be simply calculated from the subtraction of the indexes of the primary and secondary reflections as  $(h_p-h_s, k_p-k_s, l_p-l_s)=(h_t, k_t, l_t)$  (see figure 2).

The TOF experimental investigations were carried out on the linac based small accelerator cold neutron source at the Hokkaido University in Sapporo. By using the performance schematically shown in figure 4 and the flight path of about 7 m the TOF spectra were collected at the marked points (see figures 5-10) related to three chosen Si slabs of different cut. The following figures 11-17 display the obtained TOF spectra. In principle, in the case of the first two crystal slabs one could

expect to see Si(111) reflections as well as the related possible MBR effects. As no such reflections were observed, for a better visibility of other effects at shorter neutron wavelengths only parts of the spectra ending at the channel number 600 (from possible 1024) are displayed. Moreover, it is known that the shorter neutron wavelength the higher the density of reciprocal points in the reciprocal space. Consequently, also the number of pairs of secondary/tertiary reflections increases.

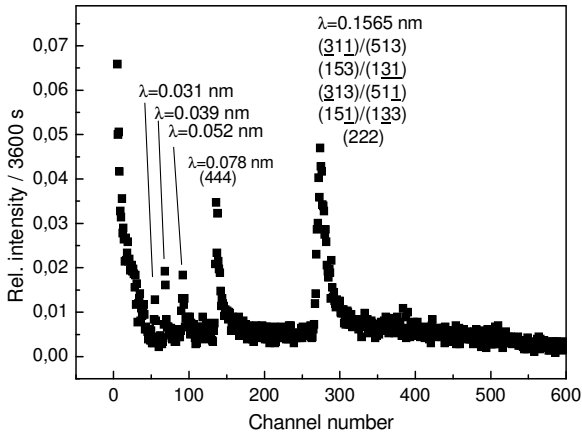


**Figure 11.** TOF spectrum taken with the bent crystal slab ( $R=8$  m) of the thickness of 3.7 mm set for forbidden Si(222) reflection at  $\theta=30^\circ$  (see figures 5 and 8).

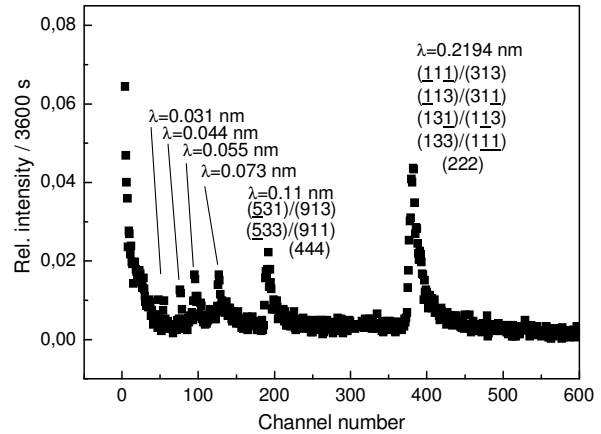


**Figure 12.** TOF spectrum taken with the bent crystal slab ( $R=8$  m) of the thickness of 3.7 mm set for forbidden Si(222) reflection at  $\theta=44.4^\circ$  (see figures 5 and 8).

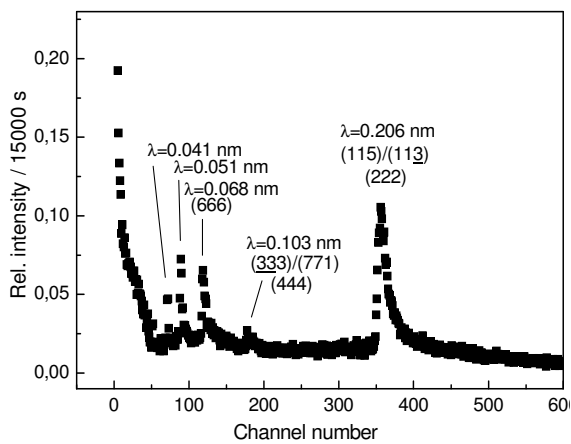


**Figure 13.** TOF spectrum taken with the bent crystal slab ( $R=10$  m) of the thickness of 4.1 mm set for forbidden Si(222) reflection at  $\theta=41^\circ$  (see figures 6 and 9).

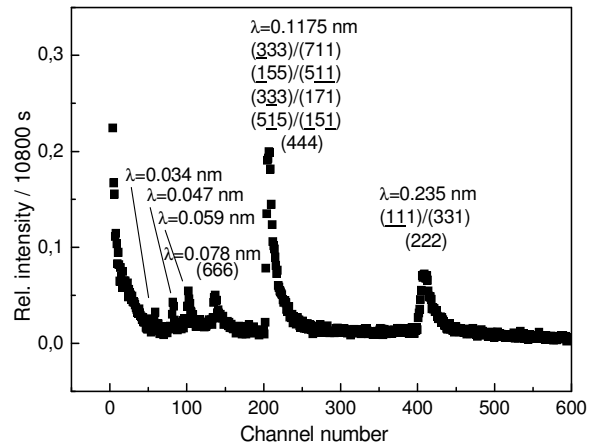


**Figure 14.** TOF spectrum taken with the bent crystal slab ( $R=10$  m) of the thickness of 4.1 mm set for forbidden Si(222) reflection at  $\theta=48.5^\circ$  (see figures 6 and 9).

Therefore, in the present case, indexing of higher order MBR-effects was not calculated but only the expected neutron wavelengths ( $\lambda/n$ ) are marked. The inspection of the figures 11-17 reveals the following effects. In all cases of figures 11-15 the forbidden Si(222) reflection is simulated by strong MBR effects and also accompanied by higher order MBR effects. However, the second order MBR effect is very weak in figure 13 and it is missing in figure 15. As the Si(444) reflection is allowed, it also means that its contribution due to the symmetric transmission geometry is very small which

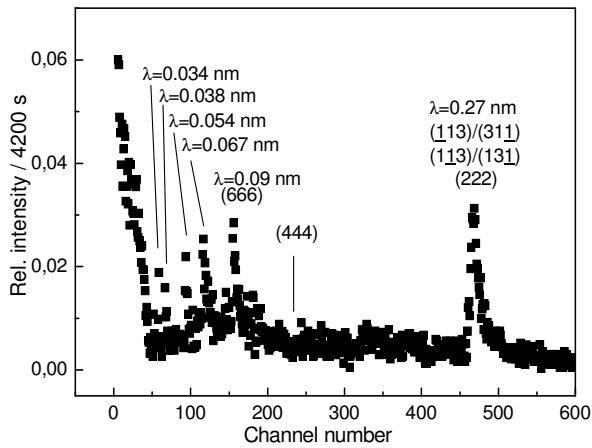


**Figure 15.** TOF spectrum taken with the bent crystal slab ( $R=10$  m) of the thickness of 4.1 mm set for forbidden Si(222) reflection at  $\theta=59.5^\circ$  (see figures 6 and 9).

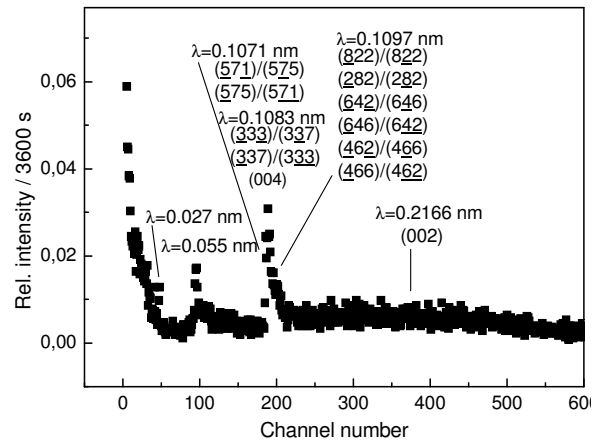


**Figure 16.** TOF spectrum taken with the bent crystal slab ( $R=10$  m) of the thickness of 4.1 mm set for forbidden Si(002) reflection at  $\theta=23.5^\circ$  (see figures 7 and 10).

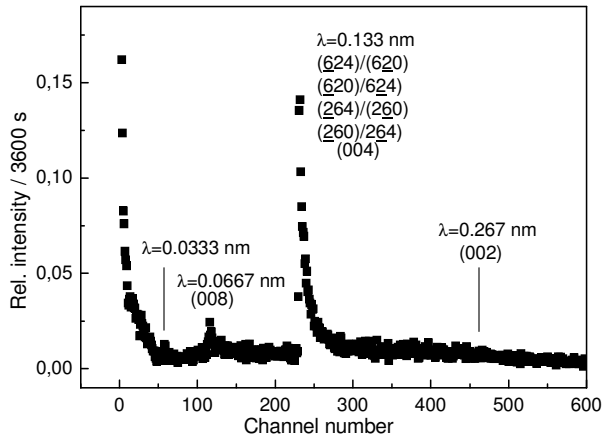


**Figure 17.** TOF spectrum taken with the bent crystal slab ( $R=10$  m) of the thickness of 4.1 mm set for forbidden Si(002) reflection at  $\theta=29.5^\circ$  (see figures 7 and 10).

corresponds to a perfect nondeformed crystal (see the text in the former paragraph). On the other hand in the case of searching the MBR effect with respect to the forbidden Si(002) reflection, none was observed. But second orders MBR effects accompanying allowed Si(004) reflection are very strong.

#### 4. Summary

On the basis of the obtained experimental results it can be stated that the MBR-effects could be considerably strengthened by elastic deformation and can be investigated by the TOF method even at small accelerator based neutron sources. TOF spectra allow us to distinguish contributions of higher orders from the first order. Thanks to homogeneous elastic deformation of the perfect single crystal the double diffraction process can be simply

assumed as a diffraction by a bicrystal system consisting of two different (deformed) single crystals mutually in the dispersive setting. As has been already tested at the steady state sources, the double diffracted beam is highly monochromatic and highly collimated. The double diffracted beam may have the cross-section of several square centimetres. Strong MBR effects can be used e.g. in high resolution neutron diffractometry, in neutron radiography, for precise determination of the neutron wavelength and thus for a possible spectroscopic characterisation of neutron sources. On the other hand, MBR effects can bring about severe limitations in precise structural investigations, namely when elastically deformed crystals are used as samples.

#### Acknowledgements

Bragg diffraction optics investigations are in the Czech Republic supported by GACR project no. 14-36566G, by the ESS project LM2010011: ‘Contribution to Partnership in Large Research Infrastructure of Pan-European Importance’ as well as by the project of EU-FP7-NMI3 II: ‘Integrated Infrastructure Initiative for Neutron Scattering and Muon Spectroscopy’, 2009-2015.

## References

- [1] Ewald P P 1937 *Z. Kristallogr.* **A97** 1.
- [2] Renninger M 1960 *Z. Kristallogr.* **113** 99.
- [3] Pinsker Z G 1978 *Dynamical Scattering of X-rays in Crystals*. Berlin: Springer-Verlag.
- [4] Chang S H 1984 *Multiple Diffraction of X-rays in Crystals*, Springer Verlag, Berlin; 1987 Moscow, Mir (Russian translation).
- [5] Moon R and Shull C G 1964 *Acta Cryst.* **17** 805.
- [6] Kuich G and Rauch H 1965 *Acta Phys. Austriaca* **20** 7.
- [7] Kuich G and Rauch H 1967 *Nukleonik* **9** 139.
- [8] Thomson P and Grimes N V 1977 *J. Appl. Cryst.* **10** 369.
- [9] Seong B S, Shin E, Lee C H, Em V T and Shim H S 2001 *J. Neutron Res.* **9** 363.
- [10] Mikula, P., Michalec, R.T., Vrána, M. and Vávra, J 1979 *Acta Cryst. A* **35** 962.
- [11] Mikula P, Vrána M, Michalec R T, Kulda J and Vávra J 1980 *Phys. Stat. Sol.(a)* **460** 549.
- [12] Vrána M, Mikula P, Michalec R T, Kulda J and Vávra J 1981 *Acta Cryst. A* **37** 459.
- [13] Mikula P, Kulda J, Vrána M, Michalec R T. and Vávra J 1982 *Nucl. Instrum. Methods* **197** 563.
- [14] Mikula P, Vrána M and Wagner V 2004 *Physica B* **350** e667.
- [15] Mikula P, Vrána M and Wagner V 2006 *Z. Kristallogr. Suppl.* **23** 205.
- [16] Mikula P, Vrána M, Šaroun J, Seong B S, Em V and Moon M K 2011 *Nucl. Instrum. Methods in Phys. Res. A*, **634** S108.
- [17] Mikula P, Vrána M, Šaroun J, Em V, Davydov V and Seong B S 2012 *J. Appl. Cryst.* **45** 98.
- [18] Kulda J and Mikula P 1985 *Phys. Stat. Sol. (a)* **92** 95.
- [19] Takagi S 1969 *J. Phys. Soc. Japan* **26** 1239.
- [20] Mikula P, Kulda J, Vrána M and Chalupa B 1984 *J. Appl. Cryst.* **17** 189.
- [21] Alexandrov Yu A, Eichhorn F, Kulda J, Lukáš P, Machekhina T A, Michalec R, Mikula P, Sedláková L N and Vrána M 1988 *Physica B* **151** 108.
- [22] Cole H, Chambers F W and Dun H M 1962 *Acta Cryst.* **15** 138.
- [23] Kotwitz D A 1968 *Acta Cryst.* **A24** 117.